On the modeling of sound transmission through a mixed separation of flexible structure with an aperture

Xiang Yu and Li Cheng[a)]
Department of Mechanical Engineering, The Hong Kong Polytechnic University, Hung Hom, Kowloon, Hong Kong, Hong Kong Special Administrative Region

Jean-Louis Guyader
Laboratoire Vibrations-Acoustique, INSA Lyon, 25 bis, avenue Jean Capelle, 69621 Villeurbanne Cedex, France

(Received 26 July 2013; revised 10 November 2013; accepted 27 March 2014)

Modeling sound transmission among acoustic media through mixed separations, consisting of both rigid/flexible structures with apertures, is a challenging task. The coexistence of both structural and acoustic transmission paths through the same coupling surface adds system complexities, hampering the use of existing sub-structuring modeling techniques when the system configuration becomes complex. In the present work, a virtual panel treatment is proposed to model thin apertures involved in such complex vibroacoustic systems. The proposed virtual panel considers an aperture as an equivalent structural component, which can be integrated with the solid/flexible structure to form a unified compound interface. This allows handling the entire compound interface as a pure structural element, thus providing an efficient and versatile tool to tackle system complexities when using sub-structuring techniques. The accuracy and convergence of the method are investigated and validated, and the effective thickness range allowing for the virtual panel treatments is determined. The capability and the flexibility of the proposed formulation are demonstrated through several numerical examples, with underlying physics being explored.
© *2014 Acoustical Society of America*. [http://dx.doi.org/10.1121/1.4870707]

PACS number(s): 43.55.Fw, 43.55.Rg, 43.20.Tb [JES] Pages: 2785–2796

I. INTRODUCTION

The sound transmission through structures is strongly affected by the presence of apertures. Typical examples include enclosures with partial partitions, holes and slits on walls, rooms with ventilation ducts for air circulation, mufflers with apertures, etc. Despite the persistent effort made in predicting the effect of an aperture of either negligible or finite thickness, sound transmission between acoustic media through a mixed separation/interface consisting of both structures and apertures has seldom been considered in the literature.

It is the aim of this paper to propose a modeling technique to deal with such systems involving a mixed separation/interface as illustrated in Fig. 1. The interface, connecting the two acoustic domains I and II, may comprise a structure that can be either rigid or flexible and an aperture that is acoustically transparent. The acoustic domains on both sides of the interface can be of any type, open or closed, although enclosures are used in Fig. 1 for illustration purposes. While the flexible structure transmits sound through its flexural vibration, the aperture allows direct acoustic coupling between the two acoustic media and usually becomes the dominant sound transmission path when it reaches a certain size.

In the absence of an aperture, the sound transmission through a complete structure has been extensively discussed in the open literature using various methods.[1–6] For example, Dowell *et al.*[1] proposed an acoustoelasticity framework to deal with the general problem of acoustic enclosures coupled to vibrating structures. One of the most used configurations is a rectangular acoustic cavity coupled to a flat flexible wall.[2] Cheng and Nicolas[3] studied the internal sound field inside a cylindrical shell with the consideration of the structural-fluid coupling with an end plate. Pan *et al.*[4,5] investigated the sound transmission into an enclosure through a vibrating plate using active noise control technique. The commonality among all this work is the involvement of a closed structural boundary that completely separates the two adjacent acoustic domains. In such a case, the coupled system can be conveniently divided into structural and acoustical subsystems, and the coupling between them is performed by applying corresponding continuity conditions along the boundaries. However, when the separation is partially covered by the structure, thus leaving an aperture, the system cannot be directly modeled using the above formulations.

On the other hand, an earlier attempt on the modeling of a complete opening was made by Dowell *et al.*,[1] who investigated the natural modes of multiple cavities, connected through completely opened air opening in between, being modeled as a flexible member with zero mass and stiffness. Later on, sound transmission through a pure aperture being inserted onto a rigid baffle or wall was studied.[7–15] For example, Guyader *et al.*[7,8] predicted the acoustic field inside a cavity with a partial or holed plate. Gomperts and Kihlman[11] calculated the sound transmission coefficient of

a)Author to whom correspondence should be addressed. Electronic mail: li.cheng@polyu.edu.hk

Redistribution subject to ASA license or copyright; see http://acousticalsociety.org/content/terms. Download to IP: 158.132.172.70 On: Sat, 10 May 2014 10:08:28

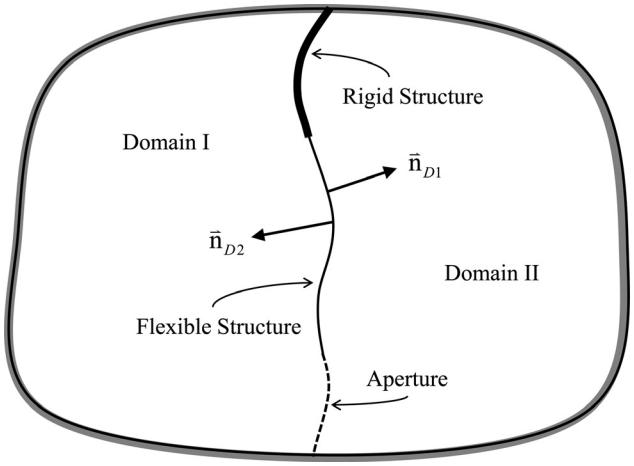

FIG. 1. General description of the problem. A mixed separation interface, consisting of rigid, flexible structures and apertures, and connecting acoustic domains I and II.

an aperture with circular or slit shape. Mechel[12] discussed the noise reduction through walls with holes and slits from architectural perspective, with sound propagation inside the holes being expressed as a superposition of two oppositely traveling plane waves. Sgard *et al.*[13,14] conducted a comprehensive review on several other similar models and investigated the transmission loss in a diffuse field for some aperture dimensions.

It is observed that the above-mentioned work all addresses a relatively simple vibroacoustic system. In principle, an aperture could possibly be modeled by means of the propagating and evanescent acoustic waves as reviewed in references.[12–15] In this way, the mixed separation/interface could be modeled as partially structural plus a pure acoustical component. One obvious disadvantage is that the modeling procedure could quickly become too tedious to be implemented when more partial separations are present. For example, when Huang *et al.*[16] studied a staggered double glazed ventilation window system using a similar approach, the acoustic domain had to be divided into five sub-domains, thus requiring the description of ten sets of continuity equations with ten unknown modal coefficient vectors to be solved. It becomes obvious that the complexity of the conventional treatment restricts its capability in handling more complex systems, which will become even more troublesome when system optimization is required.

In a broader sense, dealing with complex systems to meet the need for design and optimization is still a challenge. One of such complexities may come from the presence of clusters of structural/acoustic components connected or coupled together with possible apertures in between, forming a so-called cascade system. Among existing methods, those based on sub-structuring principle are still deemed the most suitable for dealing with such structural complexity. Typical methods include impedance and mobility approach,[17] transfer matrix method,[18] and more recently, the Patch Transfer Function (PTF) approach.[19–21] The commonality among these methods is the prior handling of subsystems before assembling them together through the connecting interfaces. Cascade systems with sub-structures connected in series can be best handled by these methods. In that case, the treatment of either structural or acoustic interface alone is rather straightforward through relatively simple continuity description. A mixed interface that involves vibrating structures and apertures, however, creates parallel structural and sound transmission paths over the same interface. This adds tremendous difficulties and complexities to the existing sub-structuring techniques in terms of connecting the two adjacent sub-structures together.

In the present work, a modeling technique is proposed to treat the aperture as a virtual panel element. The prerequisite of the formulation is that the aperture thickness should be small compared to the acoustic wavelength of interest, so that the transverse acoustic velocity across the aperture thickness undergoes negligible variations. By considering the aperture as an equivalent structural component, which will be referred to as virtual panel hereafter, this treatment allows handling mixed interface in a more efficient way, especially when packaged as a subsystem module under the sub-structuring modeling framework. The unification of the structural and acoustic sound transmission paths into a single structural one, to be described by a compound mobility matrix, provides an effective means to deal with vibroacoustic systems involving complex mixed separations. As such, the proposed technique is expected to facilitate the sub-structuring treatment of complex vibro-acoustic systems. It should, therefore, be regarded as a key step in the development of the sub-structuring techniques and an alternative to other existing methods. Typical intended applications include the design of silencers, multilayer ventilation windows, vehicle cabins, or rooms with internal partial partitions, etc.

In this paper, the modeling of the virtual panel together with the traditional interface treatment (matching the pressures and velocities at the boundaries) is first formulated. In fact, the virtual panel is based on the interface treatment of a general aperture of an arbitrary thickness, and is regarded as a particular case when the thickness is small (illustrated in Fig. 2). The accuracy of the two treatments is then assessed and validated through comparisons with finite-element method (FEM) analyses, using an acoustic cavity with internal partial obstacle. The effective thickness range allowing for the virtual panel treatment is then determined. As an example, the sound field inside a duct, segmented by four staggered partial partitions is examined, and the influences of flexible separation and a micro-perforated partition (MPP) inside a cavity are investigated. To further illustrate the capability of the proposed method in handling system complexities, a dual-chamber duct silencer with rigid or micro-perforated side-branch partitions is investigated, whereby the flexibility and computational efficiency of the proposed method will be demonstrated.

II. FORMULATION

Figure 2 shows a generic system which consists of two acoustic media separated by a partial structure with an aperture. The aperture in the present case is the air volume bounded by the structure with a thickness of L_z as shown in Fig. 2(a). The sound pressure inside the aperture, $p_o(x, y, z)$, can be expressed as

Redistribution subject to ASA license or copyright; see http://acousticalsociety.org/content/terms. Download to IP: 158.132.172.70 On: Sat, 10 May 2014 10:08:28

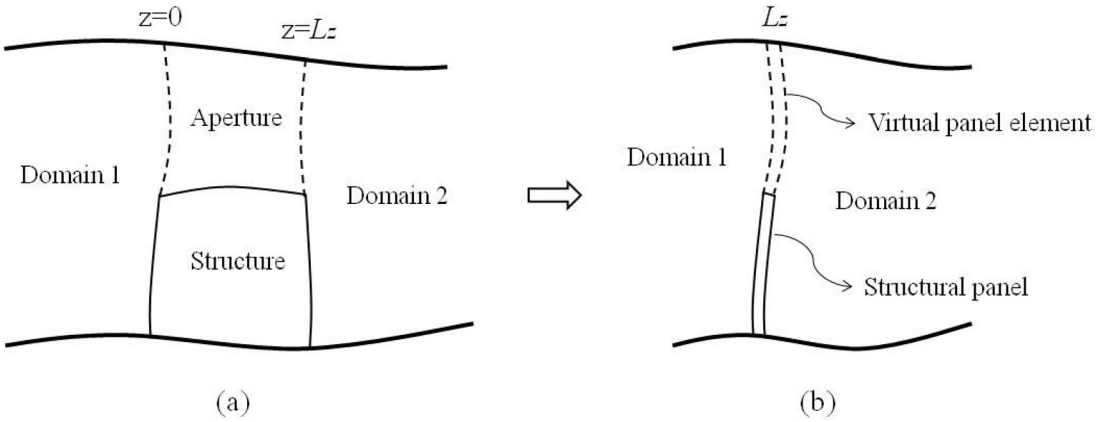

FIG. 2. Two formulations. (a) Traditional interface treatment for aperture with arbitrary thickness. (b) Virtual panel treatment for aperture with small thickness.

$$p_o(x,y,z)=\sum_{st}(\hat{A}^{st}e^{-jk_z^{st}z}+\hat{B}^{st}e^{jk_z^{st}z})\psi_o^{st}(x,y), \tag{1}$$

where $\hat{A}^{st}$ and $\hat{B}^{st}$ are the modal coefficients for the acoustic waves propagating in the positive and negative z directions, respectively; ψ_o^{st} is the acoustic modal shape functions in the x-y plane; $k_z^{st}=\sqrt{(\omega/c_0)^2-(k_x^s)^2-(k_y^t)^2}$ is the corresponding wavenumber along the z-axis, where k_x^s and k_y^t are subjected to the actual planar eigenfunctions.

The conventional interface treatment can be performed by establishing a set of continuity equations of pressures and velocities at the coupling interfaces, taking the coupled acoustic domains on both sides into account. According to the notations of normal directions for acoustic domains *D1* and *D2* in Fig. 1, for the coupling surface denoted by S_1, connecting the acoustic domain D_1 on the left-hand side, one has

$$\begin{cases} p_{D1}=p_o \text{ over } S_1 \text{ at } z=0 \\ \dfrac{\partial p_{D1}}{\partial z}=\dfrac{\partial p_o}{\partial z} \text{ over } S_1 \text{ at } z=0, \text{ and } \dfrac{\partial p_{D1}}{\partial z}=\dfrac{\partial p_o}{\partial n_{D1}}. \end{cases} \tag{2}$$

Similarly, for the coupling interface denoted by S_2, connecting the acoustic domain D_2 on the right-hand side,

$$\begin{cases} p_o=p_{D2} \text{ over } S_2 \text{ at } z=L_z \\ \dfrac{\partial p_o}{\partial z}=\dfrac{\partial p_{D2}}{\partial z} \text{ over } S_2 \text{ at } z=L_z, \text{ and } \dfrac{\partial p_o}{\partial z}=-\dfrac{\partial p_{D2}}{\partial n_{D2}}, \end{cases} \tag{3}$$

where the subscripts D_1, D_2, and o denote the two acoustic media and the aperture, respectively.

Using the pressure expression in Eq. (1) in the above continuity conditions, multiplying both sides of each equation by ψ_o^{st} and integrating over the surfaces yields

$$\begin{cases} \hat{A}^{st}N_o^{st}+\hat{B}^{st}N_o^{st}=\displaystyle\int_{S_1}(p_{D1}\psi_o^{st})\,dS_1 \text{ over } S_1 \text{ at } z=0 \\ \hat{A}^{st}e^{-jk_z^{st}L_z}N_o^{st}+\hat{B}^{st}e^{jk_z^{st}L_z}N_o^{st}=\displaystyle\int_{S_2}(p_{D2}\psi_o^{st})\,dS_2 \text{ over } S_2 \text{ at } z=L_z \end{cases} \tag{4}$$

where $N_o^{st}=\int_{S_o}\psi_o^{st}\psi_o^{s't'}\,dS_o$, and the first derivatives of pressures

$$\begin{cases} \dfrac{\partial p_{D1}}{\partial z}=\displaystyle\sum_{st}jk_z^{st}(-\hat{A}^{st}+\hat{B}^{st})\psi_o^{st} \text{ over } S_1 \text{ at } z=0 \\ \dfrac{\partial p_{D2}}{\partial z}=\displaystyle\sum_{st}jk_z^{st}(-\hat{A}^{st}e^{-jk_z^{st}L_z}+\hat{B}^{st}e^{jk_z^{st}L_z})\psi_o^{st} \text{ over } S_2 \text{ at } z=L_z. \end{cases} \tag{5}$$

This interface treatment provides an accurate description of the sound field within the air volume occupied by the aperture in all directions, including the sound propagation across the thickness. Here, the aperture is treated as a purely acoustic element. The thick partial structure is considered to be rigid, which does not require special treatment.

When the partial structure becomes thin and flexible, the aperture degenerates to a thin air layer bounded by a partial flexible structure as shown in Fig. 2(b). In this case, the modeling of the structural part of the mixed separation does not present any technical problem, and that of the thin aperture requires special treatment so that it can be modeled as an

Redistribution subject to ASA license or copyright; see http://acousticalsociety.org/content/terms. Download to IP: 158.132.172.70 On: Sat, 10 May 2014 10:08:28

equivalent structural component to be integrated with its structural counterpart. Similar to Eq. (1), the pressure field at any point inside the thin aperture can still, in principle, be superposed by two oppositely propagating acoustic waves as

$$p_o(x,y,z) = \sum_{st} a_o^{st}\psi_o^{st}(e^{-jk_z^{st}z} + \varepsilon^{st}e^{jk_z^{st}z}), \tag{6}$$

where a_o^{st} is introduced as the aperture modal amplitude corresponding to the planar mode indices s, t, and the term ε^{st} is the ratio between the two previously defined modal coefficients as $\varepsilon^{st} = \hat{B}^{st}/\hat{A}^{st}$.

Assuming the aperture thickness is small enough compared to the acoustic wavelength of interest, the sound pressure in the thickness direction can be expanded by the Taylor series, with terms higher than the second order being neglected, resulting in

$$p_o(x,y,z) \approx p_o(x,y,z_0) + \frac{\partial p_o(x,y,z_0)}{\partial z}(z - z_0). \tag{7}$$

The cross-section eigenfunctions, ψ_o^{st}, are independent of the aperture thickness, and the small thickness of the air layer delimits the velocity fluctuation in the z direction. Thus, an averaged thickness-through velocity, $\bar{V}_z$, can be assumed to characterize the pressure gradient in the z direction as

$$\frac{\partial p_o}{\partial z} = -j\rho\omega\bar{V}_z, \tag{8}$$

where $\bar{V}_z$ can be determined by different mathematical simplifications. The simplest one is to use the velocity at the front plane ($z = 0$) as

$$\bar{V}_z = \frac{1}{-j\rho\omega}\frac{\partial p_o(x,y,0)}{\partial z} = \sum_{st}\frac{a_o^{st}(1-\varepsilon^{st})}{\rho c_z^{st}}\psi_o^{st}, \tag{9}$$

where $c_z^{st} = \omega/k_z^{st}$.

By incorporating Eq. (9) into Eq. (7) and relating the pressures at the front and back planes, ε^{st} can be obtained as

$$\varepsilon^{st} = \frac{\hat{B}^{st}}{\hat{A}^{st}} = \frac{jk_z^{st}L_z - 1 + e^{-jk_z^{st}L_z}}{jk_z^{st}L_z + 1 - e^{jk_z^{st}L_z}}. \tag{10}$$

The pressure gradient is related to the pressure continuity conditions at the two coupling surfaces, which gives

$$p_{D1} - p_{D2} = \sum_{st} a_o^{st}jk_z^{st}L_z\psi_o^{st}(1-\varepsilon^{st}). \tag{11}$$

Then, multiplying both sides by ψ_o^{st} and integrating over the corresponding surfaces yields

$$a_o^{st}jk_z^{st}L_z(1-\varepsilon^{st})N_o^{st} - \int_{S_o} p_{D1}\psi_o^{st}\,dS_o + \int_{S_o} p_{D2}\psi_o^{st}\,dS_o = 0. \tag{12}$$

The above equation describes the coupling between the two acoustic media through the virtual panel element. As to the vibrating structural part, it can be formulated using the well-established methods as[6,19]

$$a_p^{mn}M_p^{mn}(\omega_{mn}^2 - \omega^2) = \int_{S_p}(p_{D1}\Phi_p^{mn} - p_{D2}\Phi_p^{mn})\,dS_p, \tag{13}$$

where a_p^{mn} is the modal amplitude of the plate displacement, Φ_p^{mn} is the corresponding mode shape; the structural modal mass $M_p^{mn} = \rho_p h\int_{S_p}(\Phi_p^{mn})^2\,dS_p$, and ρ_p and h are the density and thickness, respectively, of the plate.

The modal amplitudes, a_o^{st} and a_p^{mn}, in Eqs. (12) and (13) are associated with the aperture pressure and plate flexural displacement, respectively. In viewing the aperture as an equivalent vibrating panel, the properties of the aperture and the panel are both characterized in terms of their averaged vibrating velocity as

$$\begin{aligned}
&\text{Aperture}: \ \bar{V}_z = \sum_{st}\frac{j\omega\psi_o^{st}}{\rho L_z\omega^2 N_o^{st}} \\
&\qquad\times\left(\int_{S_o} p_{D2}\psi_o^{st}\,dS - \int_{S_o} p_{D1}\psi_o^{st}\,dS\right), \\
&\text{Flexible panel}: \ \bar{V}_z = \sum_{mn}\frac{j\omega\,\Phi_p^{mn}}{M_p^{mn}(\omega^2 - \omega_{mn}^2)} \\
&\qquad\times\left(\int_{S_p} p_{D2}\Phi_p^{mn}\,dS - \int_{S_p} p_{D1}\Phi_p^{mn}\,dS\right).
\end{aligned} \tag{14}$$

It can be seen from the above expression that the modeling of the aperture can be regarded as purely structural. The equivalent structural properties of the virtual panel include: density equal to air density, ρ, panel thickness, L_z, and an frequency-dependent stiffness (not explicitly shown here). If necessary, an equivalent damping can also be introduced using a complex wavenumber $k^* = \omega/c^* = \omega/\left(c^*\sqrt{1+j\eta}\right)$, where η is the fluid damping loss factor.[19] The cross influence of the structural part on the aperture is deemed to be negligible and the edge of a thin partial structure does not require special treatment,[7] thus, the structural and virtual structural components can be formulated separately.

It should be noted again that the current formulation only focuses on the partial separation itself, while the acoustic domains on both sides can be readily treated by the existing modeling tools available in the open literature. For example, the sound field inside acoustic cavities of simple geometries can be expressed analytically in terms of modal expansions.[6,15] For cavities with other shapes, various so-called semi-analytical methods[22] or FEM/boundary-element method[23] can be employed. For semi-infinite acoustic domains, the excitation can be assumed as simple normal or oblique incident waves, and the radiated sound field can be modeled by radiation impedance matrix using Rayleigh's integral when the system is embedded in an infinite rigid baffle.[13,19]

III. VALIDATIONS AND NUMERICAL EXAMPLES

A. Validation of the interface treatment

In order to validate the proposed formulation, a system consisting of two rectangular cavities separated by a partial structure as shown in Fig. 3 is considered. The entire system contains four parts, namely, a partial obstacle, an air aperture, and two acoustic cavities on each side. The cross-section of the cavity and the aperture is chosen as rectangular shaped for the sake of simplicity, whose eigenfunctions for modal expansions are analytically known. The exterior

Redistribution subject to ASA license or copyright; see http://acousticalsociety.org/content/terms. Download to IP: 158.132.172.70 On: Sat, 10 May 2014 10:08:28

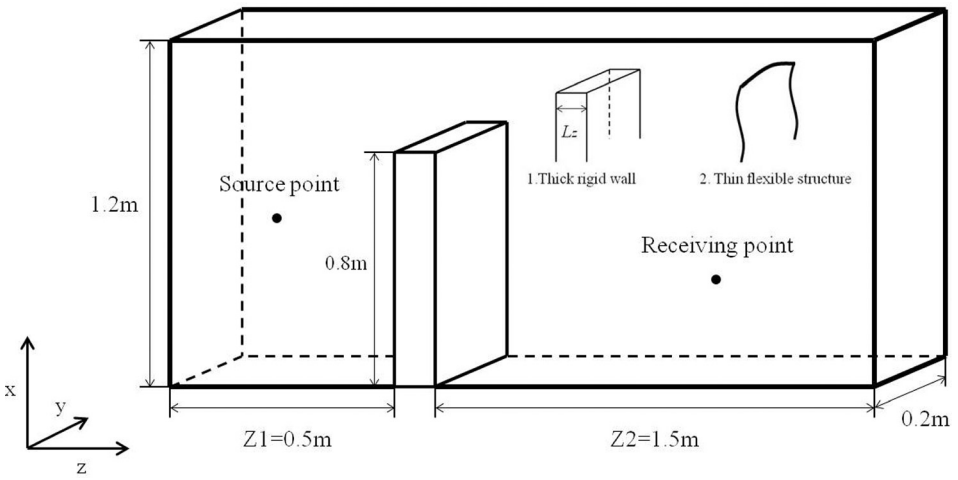

FIG. 3. A rectangular cavity with a rigid/flexible partial structure inside. Source position located at (0.6,0,0.2) m.

boundaries are taken as rigid walls and the damping loss factors for all the acoustic domains are taken as zero. The dimensions of the system are illustrated in Fig. 3.

The sound pressure fields in both cavities are expressed as modal expansions of rigid-walled acoustic cavities. The accuracy of this treatment have been extensively discussed in the literature.[24,25] If necessary, the accuracy could be improved by taking into account the pseudo-static correction for the modes which are not retained in the modal expansion.[26] This is, however, beyond the scope of the present investigation, since numerical results show that the desired accuracy can already be reached. The coupling treatment via the aperture makes use of the Green's function together with the Helmholtz equation, similar formulation procedures have been well documented in some other studies, thus, only major steps showing the modeling framework will be presented here. The coupling equation for each acoustic enclosure surrounded by a vibrating boundary is established as

$$a_e^{pqr}N_e^{pqr}(k^2-k_{pqr}^2)=\int_{s_e}\left(-\varphi_e^{pqr}\frac{\partial p_e}{\partial n}\right)dS_e - \int_{V_e}(S_0\varphi_e^{pqr}\delta_{xyz})\,dV_e, \tag{15}$$

where a_e^{pqr} is the enclosure modal amplitude identified by the modal indices p, q, r; φ_e^{pqr} are the corresponding eigenfunctions; $N_e^{pqr}=\int_{V_e}\varphi_e^{pqr}\varphi_e^{p'q'r'}\,dV_e$; S_e and V_e denote the boundary surface and interior volume; S_0 is the amplitude of the sound source placed inside the enclosure, and δ_{xyz} is the Dirac-delta.

Referring to the current configuration, the sound source is placed inside the left cavity, and the interaction through the aperture is formulated by substituting the normal pressure gradients $\partial p_{e1}/\partial n_{D1}$ and $\partial p_{e2}/\partial n_{D2}$ into Eq. (15). These two pressure gradients are found from the expressions of $\partial p_{D1}/\partial z$ and $\partial p_{D2}/\partial z$ in Eq. (5), respectively. Thus,

$$\begin{aligned}&a_{e1}^{pqr}N_{e1}^{pqr}(k^2-k_{e1}^2)-\sum_{st}jk_z^{st}(\hat{A}^{st}-\hat{B}^{st})\int_{s_1}\psi_o^{st}\varphi_{e1}^{pqr}\,dS_1\\&\quad=-\int_{V_1}(S_0\varphi_{e1}^{pqr}\delta_{xyz})\,dV_1,\\&a_{e2}^{pqr}N_{e2}^{pqr}\left(k^2-k_{e2}^2\right)+\sum_{st}jk_z^{st}(\hat{A}^{st}e^{-jk_z^{st}L_z}-\hat{B}^{st}e^{jk_z^{st}L_z})\\&\quad\times\int_{s_2}\psi_o^{st}\varphi_{e2}^{pqr}\,dS_2=0.\end{aligned} \tag{16}$$

The coupling equations for the aperture in Eq. (4) are developed using the pressure expansions of both sub-cavities

$$\begin{aligned}&\sum_{pqr}^{e1}a_{e1}^{pqr}\int_{s_1}\psi_o^{st}\varphi_{e1}^{pqr}\,dS_1=(\hat{A}^{st}+\hat{B}^{st})N_o^{st},\\&\sum_{pqr}^{e2}a_{e2}^{pqr}\int_{s_2}\psi_o^{st}\varphi_{e2}^{pqr}\,dS_2=(\hat{A}^{st}e^{-jk_zL_z}+\hat{B}^{st}e^{jk_zL_z})N_o^{st}.\end{aligned} \tag{17}$$

Now, the full system of coupling equations using continuous boundary conditions have been established and the unknown modal coefficients are to be solved. The above governing equations are condensed into matrix form as $[M]\{A\}=\{E\}$ by letting

$$\begin{aligned}&\boldsymbol{K}_1=\int_{s_1}\psi_o^{st}\varphi_{e1}^{pqr}\,dS_1\quad\text{and}\quad\boldsymbol{K}_2=\int_{s_2}\psi_o^{st}\varphi_{e2}^{pqr}\,dS_2,\\&\boldsymbol{S}_1=\int_{V_1}(S_0\varphi_{e1}^{pqr}\sigma_{xyz})\,dV_1.\end{aligned} \tag{18}$$

$\boldsymbol{M}$ is the matrix containing all the cross-coupling terms

$$\boldsymbol{M}=\begin{bmatrix}N_{e1}^{pqr}(k^2-k_{e1}^2) & -jk_z^{st}\boldsymbol{K}_1 & jk_z^{st}\boldsymbol{K}_1 & \\ -\boldsymbol{K}_1 & N_o^{st} & N_o^{st} & \\ & N_o^{st}e^{-jk_z^{st}L_z} & N_o^{st}e^{jk_z^{st}L_z} & -\boldsymbol{K}_2\\ & jk_z^{st}\boldsymbol{K}_2e^{-jk_z^{st}L_z} & -jk_z^{st}\boldsymbol{K}_2e^{jk_z^{st}L_z} & N_{e2}^{pqr}(k^2-k_{e2}^2)\end{bmatrix};$$

Redistribution subject to ASA license or copyright; see http://acousticalsociety.org/content/terms. Download to IP: 158.132.172.70 On: Sat, 10 May 2014 10:08:28

$\boldsymbol{A}$ is the modal coefficients vector

$$\boldsymbol{A} = [a_{e1}^{pqr}; \hat{A}^{st}; \hat{B}^{st}; a_{e2}^{pqr}];$$

$\boldsymbol{E}$ is the excitation source vector:

$$\boldsymbol{E} = [-\boldsymbol{S}_1; \mathbf{0}; \mathbf{0}; \mathbf{0}].$$

The validity of the interface treatment is tested by first focusing on a thick aperture case with $L_z = 0.2$ m, with the structural vibration being naturally neglected. Since this configuration has no analytical solution available for referencing purpose, the calculated results using the present approach are validated against FEM simulation performed by using commercial FEM software COSMOL Multiphysics, which solves the problem in physical (nodal) coordinates. More specifically, the pressure field inside the cavity is excited by a point source placed in the left sub-cavity at $(0.6, 0, 0.2)$ m, the sound pressure level (SPL) at the observation point $(0.4, 0, 1.7)$ m is to be examined. For the present approach, care was taken to include a sufficient number of modes in the calculation to ensure the convergence of the calculation, on one hand, and, on the other hand, to avoid excessively higher order modes whose eigenfrequencies are several times greater than the frequency range of interest. For the current study, the truncation frequency is taken as 4000 Hz, which can guarantee the convergence of the calculation below 2000 Hz.

The natural frequencies of the coupled system correspond to the peaks on the predicted SPL curves. In Table I, the natural frequencies predicted by the present approach are listed together with the results provided by FEM simulation. In total, 16 resonances below 400 Hz are compared with the percentage errors being calculated. The predicated results show almost perfect agreement with the FEM ones, with maximum frequency discrepancies of less than 0.5 Hz.

Next, the SPL curves from the present approach and FEM at the receiving point are compared. As shown in Fig. 4, the natural resonances can be easily identified from the sharp peaks, and the two SPLs match well within the entire frequency range albeit some tiny discrepancies. The discrepancies may possibly be due to the selected modal basis for the sub-cavity pressure expansions, where the assumed rigid-walled acoustic modes may slightly differ from the real situation at some frequencies. This phenomenon also appears in the work reported by Dowell,[1] in which the actual eigenfunctions of the cavity in presence of the coupled aperture were shown to differ from that of the rigid-walled cavity. Despite this, the accuracy of the interface treatment for the thick aperture is deemed very satisfactory.

TABLE I. Validation of the interface treatment. Coupled system resonances predicted from the present approach compared with FEM, $L_z = 0.2$ m.

Mode	Calculated	FEM	Error (%)	Mode	Calculated	FEM	Error (%)
1	0	0	0	9	283.8	283.5	0.11
2	53.8	53.8	0	10	291.4	291.3	0.03
3	117.6	117.4	0.17	11	306.6	306.8	−0.06
4	138.8	138.5	0.22	12	324.7	324.7	0
5	158.3	158.3	0	13	349.4	349.4	0
6	194.5	194.5	0	14	356.4	356.4	0
7	230.8	230.5	0.13	15	365.6	365.4	0.05
8	264.7	264.6	0.04	16	399.5	399.0	0.125

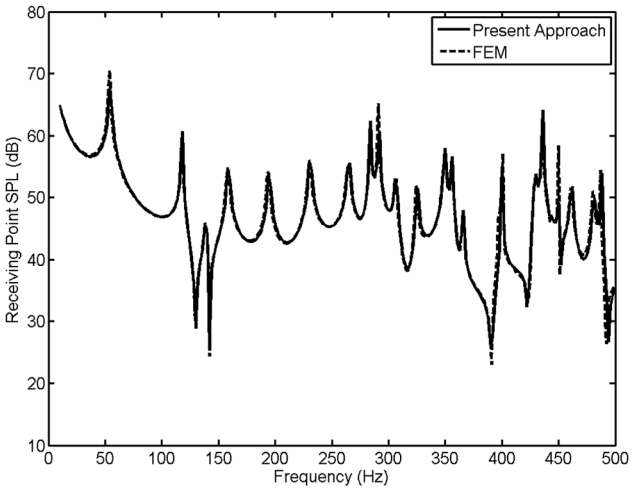

FIG. 4. Validation of the interface treatment. Comparison of SPLs at the receiving point between the present approach and FEM, rigid partial structure with thickness $L_z = 0.2$ m.

B. Validation of the virtual panel treatment

The convergence of the virtual panel treatment will be verified with the depth of the previous aperture reduced to $L_z = 0.002$ m. The formulation procedure for the subdivided acoustic cavities is identical as before, whereas the coupling via the compound separation is treated by replacing the arbitrary acoustic domains, $D1$ and $D2$, in Eq. (12) with the pressure fields of both rectangular sub-cavities as

$$a_o^{st} jk_z^{st} L_z (1 - \varepsilon^{st}) N_o^{st} - \sum_{pqr}^{e1} a_{e1}^{pqr} \int_{S_o} \varphi_{e1}^{pqr} \psi_o^{st} \, dS_o + \sum_{pqr}^{e2} a_{e2}^{pqr} \int_{S_o} \varphi_{e2}^{pqr} \psi_o^{st} \, dS_o = 0. \tag{19}$$

Also, the equation that governs the coupling via the vibrating structure is

$$a_p^{mn} M_p^{mn} (\omega_{mn}^2 - \omega^2) - \sum_{pqr}^{e1} a_{e1}^{pqr} \int_{s_p} \varphi_{e1}^{pqr} \Phi_p^{mn} \, dS_p + \sum_{pqr}^{e2} a_{e2}^{pqr} \int_{s_p} \varphi_{e2}^{pqr} \Phi_p^{mn} \, dS_p = 0. \tag{20}$$

Using a similar technique, the above coupling equations are condensed into matrix form as $[M']\{A'\} = \{E'\}$, with extra coupling terms for the structure being specified as

$$\boldsymbol{L}_1 = \int_{s_p} \varphi_{e1}^{pqr} \Phi_p^{mn} \, dS_p \quad \text{and} \quad \boldsymbol{L}_2 = \int_{s_p} \varphi_{e2}^{pqr} \Phi_p^{mn} \, dS_p. \tag{21}$$

The new matrix $\boldsymbol{M}'$ containing all the cross-coupling terms is

Redistribution subject to ASA license or copyright; see http://acousticalsociety.org/content/terms. Download to IP: 158.132.172.70 On: Sat, 10 May 2014 10:08:28

$$\boldsymbol{M}' = \begin{bmatrix} N_{e1}^{pqr}(k^2 - k_{e1}^2) & -jk_z^{st}\boldsymbol{K}_1(1-\hat{\varepsilon}_{st}) & \mathbf{0} & \rho\omega^2\boldsymbol{L}_1 \\ -\boldsymbol{K}_1 & jk_z^{st}L_z N_o^{st}(1-\hat{\varepsilon}_{st}) & \boldsymbol{K}_2 & \mathbf{0} \\ \mathbf{0} & jk_z^{st}\boldsymbol{K}_2(1-\hat{\varepsilon}_{st}) & N_{e2}^{pqr}(k^2 - k_{e2}^2) & -\rho\omega^2\boldsymbol{L}_2 \\ -\boldsymbol{L}_1 & \mathbf{0} & \boldsymbol{L}_2 & M_p^{mn}(\omega_{mn}^2 - \omega^2) \end{bmatrix};$$

the modal coefficients vector $\boldsymbol{A}'$ is

$$\boldsymbol{A}' = [a_{e1}^{pqr}; a_o^{st}; a_{e2}^{pqr}; a_p^{mn}];$$

and the excitation vector $\boldsymbol{E}'$ is

$$\boldsymbol{E}' = [-\boldsymbol{S}_1; \mathbf{0}; \mathbf{0}; \mathbf{0}].$$

To focus on the thin aperture itself, the partial structure is still taken as rigid, which can be simply achieved by assigning large values to the structural rigidity and density. Similar to the previous validation, the resonances predicted using the present approach are tabulated and compared with FEM simulation in Table II. It can be seen that the overall agreement is again quite good, with acceptable relative errors.

The SPLs at the receiving point calculated using the present approach and FEM simulation are compared in Fig. 5. Since the aperture thickness is decreased as compared to the configuration used in Sec. III A, the receiving point is now relocated to $(0.4, 0, 1.5)$ m. Again, the two curves match well despite a few tiny differences, which may due to the same reason as explained before.

It is relevant to note the influence of the aperture thickness on the system resonances (Tables I and II). Note that in both cases, the dimension of the sub-cavities remains the same, while the aperture thickness is changing. It is observed that a smaller aperture thickness induces higher system natural frequencies, which can be explained by the intermodal coupling with smaller volumetric mass in the thin aperture case. The influence of the partial obstacle on modifying the original pressure field of an empty cavity can also be seen, by looking at a rectangular hard-walled cavity with the same outer dimension as 1.2 m $(x) \times 0.2$ m $(y) \times 2$ m (z), tabulated in Table III. Compared with Table II, it can be seen that the partial structure obviously affects the original modal behavior of the cavity. Due to the presence of the partition, the original cavity is partially segmented, thus forming an air volume like a bended conduit around the partition and the cavity wall. Therefore, the effective length of the air volume in the cavity exceeds that of the original cavity (2 m), which can be estimated by taking the two triangle side lengths formed by the partition and the cavity base: $\sqrt{0.5^2 + 0.8^2} + \sqrt{1.5^2 + 0.8^2} = 2.7$ m. Owing to this, the first cavity resonant frequency is lowered to 62.8 Hz. Meanwhile, additional resonances are also created, dominated by the local reflection between the cavity wall and the partition. For the unobstructed x direction, the modes $(1, 0, 0)$ and $(2, 0, 0)$ are not affected, as expected.

TABLE II. Validation of the virtual panel treatment. Coupled system resonances predicted from the present approach compared with FEM, $L_z = 0.002$ m.

Mode	Calculated	FEM	Error (%)	Mode	Calculated	FEM	Error (%)
1	0	0	0	9	283.4	283.4	0
2	62.8	62.3	0.80	10	292.8	292.8	0
3	121.1	120.9	0.17	11	313.4	312.8	0.19
4	141.6	141.6	0	12	340.3	340.3	0
5	165.2	164.4	0.49	13	352.8	352.8	0
6	202.4	202	0.20	14	366	365.7	0.08
7	239.4	238.4	0.42	15	368.6	368.6	0
8	276.9	276.7	0.07	16	424	423.3	0.17

C. Effective thickness range for the virtual panel treatment

In the previous sections, the validity of the two treatments has been verified separately. The virtual panel treatment is formulated based on the assumption that the thickness of the air layer is small compared to the wavelength of interest. Thus, it is important to define an effective thickness criterion, to ensure the validity of the proposed virtual panel treatment. Due to the lack of analytical solutions, the interface treatment, already validated in Sec. III A, is used as the benchmark to test the convergence of the virtual panel treatment.

In principle, the aperture thickness criterion is related to the minimum acoustic wavelength of interest. A hypothesis is brought forward by looking into an example of the pressure field inside a rectangular cavity, which has been

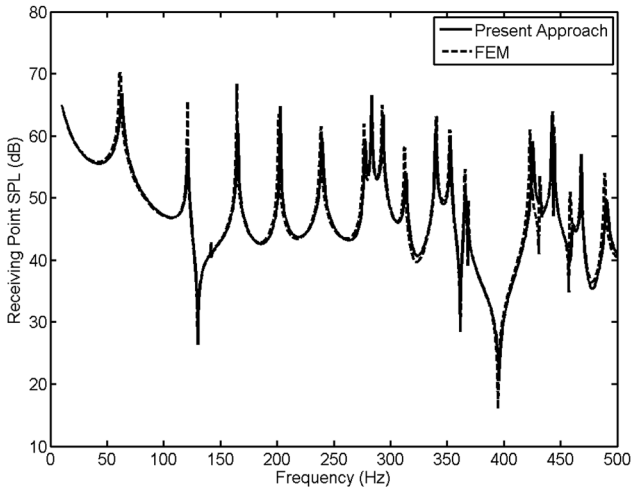

FIG. 5. Validation of the proposed virtual panel treatment. Comparison of the SPLs at the receiving point obtained from the virtual panel formulation and FEM, rigid separation with thickness $L_z = 0.002$ m.

Redistribution subject to ASA license or copyright; see http://acousticalsociety.org/content/terms. Download to IP: 158.132.172.70 On: Sat, 10 May 2014 10:08:28

TABLE III. Natural frequencies of an unobstructed empty cavity with corresponding modal indices.

Mode	Indices	Frequency	Mode	Indices	Frequency
1	(0,0,0)	0	6	(1,0,2)	221.2
2	(0,0,1)	84.9	7	(0,0,3)	254.7
3	(1,0,0)	141.7	8	(2,0,0)	283.3
4	(0,0,2)	165.2	9	(1,0,3)	291.5
5	(1,0,1)	169.8	10	(2,0,1)	295.8

discussed experimentally by Kim and Kim.[27] When the cavity dimensions are small enough, the pressure distribution inside the cavity is rather uniform, since even the first natural frequency is far beyond the frequency range of interest. Therefore, to limit the velocity variation across the aperture thickness, an intuitive guess would be that its thickness should be shorter than a quarter of minimum wavelength. For illustration purposes, the accuracy of the virtual panel treatment is tested by first taking its thickness as $\lambda_s/4 = 0.0425$ m for a frequency range up to $f = 2000$ Hz, where $\lambda_s = c_0/f$ is the minimum wavelength of interest. In Fig. 6, the calculated SPL at the receiving point is compared to the benchmark result. The agreement between two curves can be observed, suggesting that a thickness of $\lambda_s/4$ can actually provide satisfactory accuracy.

In order to systematically demonstrate the dependence of the accuracy on virtual panel thickness, a percentage error (PE) is defined as

$$\mathrm{PE} = (P_{vp} - P_{it})/P_{it} \tag{22}$$

where P_{vp} and P_{it} are the integrated areas under the sound pressure spectra obtained from virtual panel treatment and the benchmark result, respectively. For each term and every thickness to be tested, 500 frequency points of the sound pressure spectrum are linearly sampled from 10–2000 Hz. A total of 200 aperture thicknesses ranging from 0.001 m to 0.1 m are tested, and the calculated PEs are presented in Fig. 7. As expected, the convergent tendency is observed when the thickness gradually reduces, and the PE is roughly stabilized at ~0.2% after $L_z = 0.01$ m. This shows that convergence can be fully guaranteed for aperture thickness to fall into millimeter range for the present cavity configuration. In a general case, this roughly corresponds to $\lambda_s/16$, with λ_s being wavelength of the maximum frequency to be covered. In summary, although the criterion of $\lambda_s/4$ can already provide satisfactory accuracy, a thinner panel thickness up to $\lambda_s/16$ should be used to guarantee fully converged numerical results. Typically, for the aperture involved in a mixed interface with thickness in millimeter range, this corresponds to a maximum frequency up to 8.5 kHz, and 2.5 kHz, respectively.

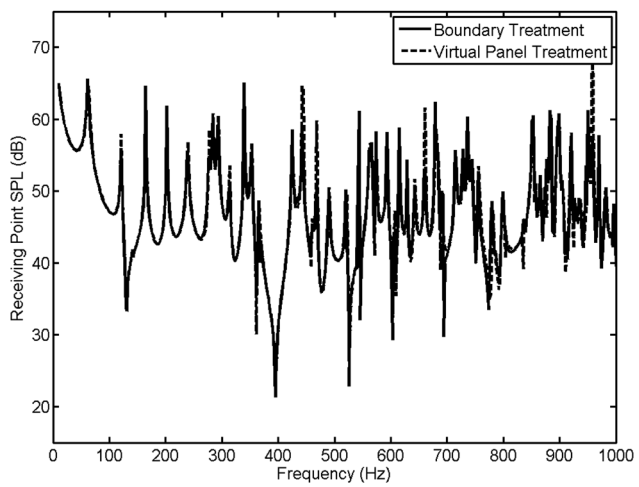

FIG. 6. Virtual panel thickness criterion test. SPLs at the receiving point; the thickness of the aperture equal to a quarter of minimum wavelength with $L_z = 0.042$ m.

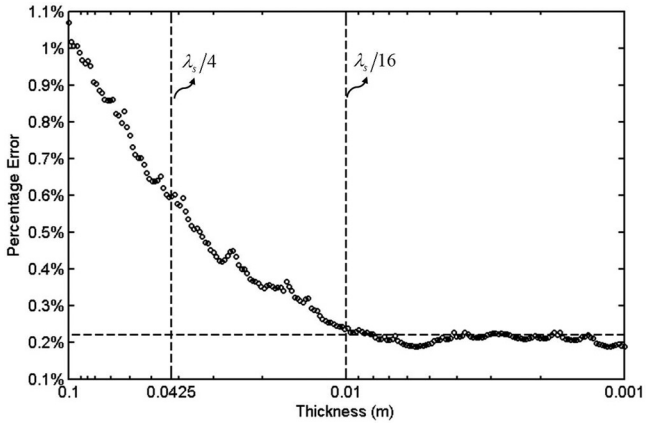

FIG. 7. Virtual panel thickness criterion test. Percentage error versus virtual panel thickness. Convergence can be fully guaranteed when $L_z \le \lambda_s/16$.

D. A duct with staggered partial partitions

The virtual panel treatment provides the flexibility to handle more complex systems such as cascade partial structures. A rectangular duct, divided into five segments by four staggered partial partitions as shown in Fig. 8(a), is used as an example to show the potential offered by such treatment. The partitions are assumed to be acoustically rigid in the simulation. The configuration involves four mixed/compound interfaces, mutually coupled through the acoustic subcavities in between, forming a typical cascade system connected in series.

In Fig. 9, the averaged SPLs inside the two sub-cavities on both ends of the duct are calculated, with peaks corresponding to the natural frequencies of the coupled system. Below 800 Hz, the predicted resonances have been verified against FEM analysis (not shown due to the lack of space). It can be seen that, in the low frequency range, dominated by the first several system resonances, the averaged SPLs inside both sub-cavities are quite comparable, suggesting a moderate obstruction effect of the partial partitions. At higher frequencies, however, the staggered partitions start to provide a certain amount of sound attenuation, acting similarly like a duct silencer system.

Redistribution subject to ASA license or copyright; see http://acousticalsociety.org/content/terms. Download to IP: 158.132.172.70 On: Sat, 10 May 2014 10:08:28

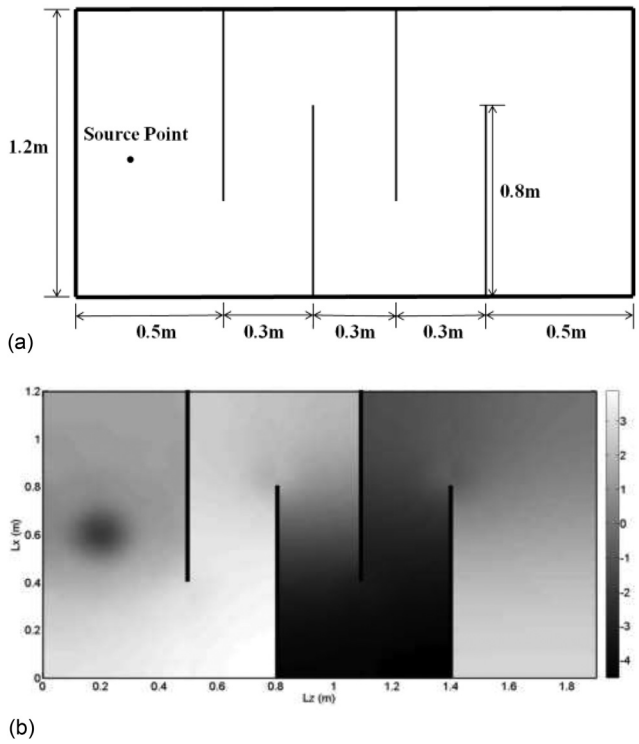

FIG. 8. A duct segmented by four staggered partial partitions. (a) Sketch of the system. (b) Visualization of the sound pressure field.

The interior sound pressure field inside the coupled acoustic domains is investigated. The calculated pressures are meshed to visualize the pressure distribution in the presence of staggered partitions. Figure 8(b) presents the gray scaled plot at $f = 100$ Hz. Referring to the arrangement of the system, the pressure variation inside the acoustic domains clearly shows the sound propagating direction. At this frequency, the sound transmission path is circuitous, with high pressure regions concentrated at the corners and conjunctions formed by the rigid structures. The sound pressures across the apertures are seen to be continuous, which proves the validity of the virtual panel element.

E. Flexible partition and MPP

Considering the configuration used in Sec. III B, a mixed separation allowing both structural and acoustic transmission paths is investigated, where the structural part can either be rigid, flexible, or micro-perforated. When the separation is flexible, an aluminum panel (thickness 2 mm, density $\rho = 2814$ kg/m^3, rigidity $E = 71e9$, Poisson's ratio $v = 0.33$, damping loss factor 0.01) is used, being assumed as simply supported along the four edges for the sake of simplicity. For other elastically supported boundaries, semi-analytical methods[28,29] are readily available to obtain the corresponding eigenfunctions for modal expansions. For the flexible partition, the first four structural resonant frequencies are calculated as 128.2 Hz, 150.8 Hz, 188.5 Hz, and 241.3 Hz.

The SPLs at the receiving point corresponding to the rigid and flexible cases are compared in Fig. 10 up to 300 Hz. As expected, the system response is strongly affected by the panel vibration within the highly dynamic range of the panel with extra peaks and dips. These extra peaks do not exactly coincide with the *in vacuo* structural resonances due to the strong structural-acoustic coupling. Within such regions, the structural transmission path has comparable importance as the acoustical path, and the sound transmission through the compound separation is a combination of both. At other frequencies where the influence of structural resonances is weak, the system resonances correspond mainly to the acoustic domains, indicating that the aperture dominates the transmission path.

The sound pressure field inside the cavity is visualized using the gray scaled plots in Fig. 11 to show the effect of the structural resonances. With a rigid partial separation, Fig. 11(a) shows the sound pressure distribution inside the cavity at 128 Hz, generated by a point source located in the left cavity. It can be observed that the sound pressure is continuous across the aperture, and the rigid wall blocks the sound transmission, evidenced by an obvious pressure jump across the partition. When the partition becomes flexible, with its first structural resonance at the same frequency of

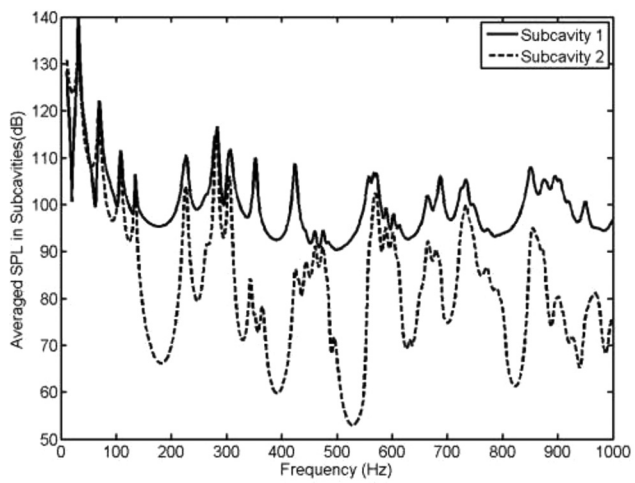

FIG. 9. A duct segmented by four staggered partial partitions. Averaged SPLs for the sub-cavities on both ends.

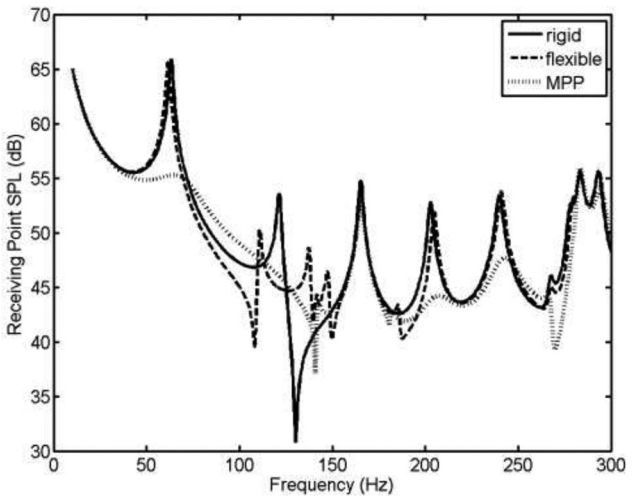

FIG. 10. Influences of flexible separation/MPP on the SPL at the receiving point.

Redistribution subject to ASA license or copyright; see http://acousticalsociety.org/content/terms. Download to IP: 158.132.172.70 On: Sat, 10 May 2014 10:08:28

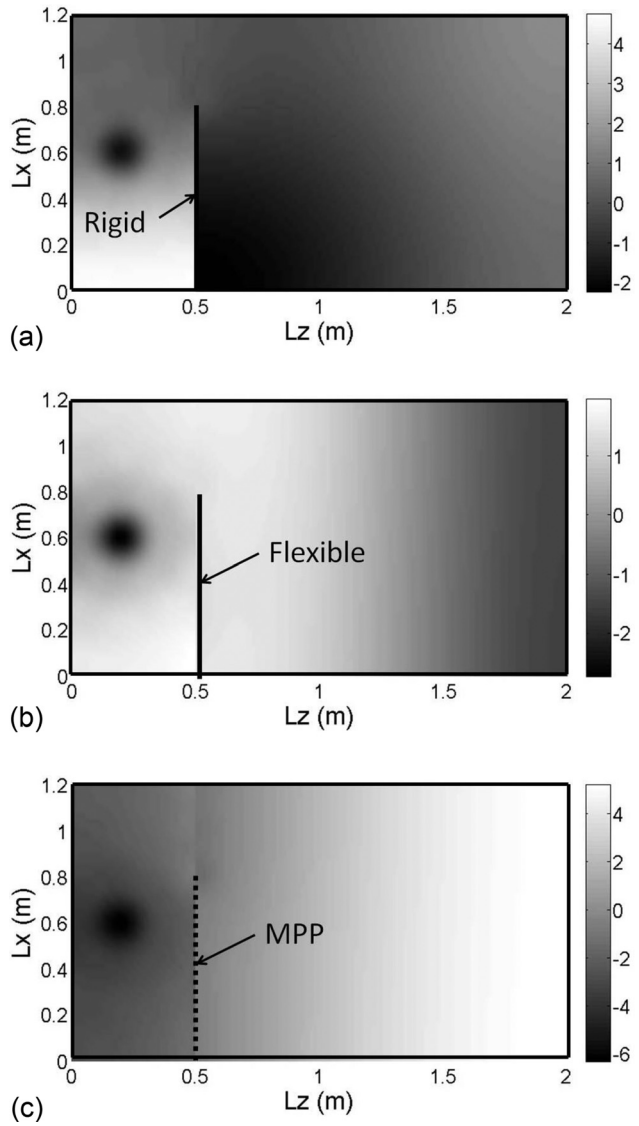

FIG. 11. Influences of flexible separation/MPP on the sound pressure distribution inside the cavity. The partial structure is (a) rigid, $f = 128.1$ Hz; (b) flexible at its first resonance, $f = 128.1$ Hz; (c) MPP, $f = 62.8$ Hz.

128 Hz, the pressure field is given in Fig. 11(b). While the pressure continuity along the aperture remains the same, the pressure jump across the structure, observed in the rigid partition case before, disappears, suggesting a significant amount of energy going through the partition via its flexural vibration. The high pressure region is no longer blocked at the bottom of the left cavity due to the low impedance of the panel at its resonances, as expected.

As to the MPP, circular holes with a diameter of 0.2 mm are uniformly distributed onto the panel surface with a perforation ratio of 1%, when the panel is deliberately kept rigid to better separate the effect. The modeling of the MPP and calculation of its characteristic impedance has been well documented in the literature;[21,30] thus, detailed modeling procedures are not repeated here. As seen from Fig. 10, the SPL at the receiving point is reduced at most of the frequencies by the introduced MPP, resulting in a more uniformed curve compared with the previous two cases. The pressure field at $f = 62.8$ Hz, corresponding to the first cavity resonance when the partition is rigid, is visualized in Fig. 11(c). It is observed that other than blocking the sound transmission, the MPP brings about a noticeable pressure balance across the partition due to the introduced small holes, which might explain the removal of the strong resonance at this frequency. The reduction of SPL typically at the cavity resonances (e.g., 62.8 Hz, 121 Hz, 202 Hz, 239 Hz) suggests that MPP adds damping to the system, by means of energy dissipation through the holes.

F. Dual-chamber duct silencer with complex internal partitions

To demonstrate the capability of the proposed virtual panel treatment in dealing with mixed separations in complex acoustic systems, the transmission loss (TL) of a dual-chamber duct silencer is considered. As shown in Fig. 12, the silencer consists of an expansion volume, being divided into two sub-chambers by a pair of rigid vertical partitions, whereas the horizontal partitions partially covering the side-branch cavities can either be solid or micro-perforated (note that further adding vibrations to these panels, perforated or not, would not add any technical difficulties). An incident plane wave is assumed at the inlet, and the outlet duct is an anechoic termination, both having a cross-section of 0.1 m × 0.1 m. The dimension of the main chamber is 0.3 m (x) × 0.1 m (y) × 0.3 m (z). The horizontal partitions (thickness 1 mm) as sketched leave apertures at the inlet/outlet ends. The MPPs have a 0.2 mm hole diameter and 1% perforation ratio. Taking advantage of the substructuring modeling framework (PTF approach) as mentioned in the Introduction, each mixed separation is characterized as a single and unified interface, in order to facilitate the coupling between subdivided acoustic domains.

When the side-branch partitions are all rigid, the predicted TL is plotted in Fig. 13, which exhibits strong resonant pattern due to the partially covered side-branch cavities as acoustic resonators.[31] For validation purpose, the same three-dimensional configuration has been considered using FEM analysis (without micro-perforation), which shows good agreement with the present approach. As to the calculation efficiency, FEM analysis solves the entire system with 5×10^5 degrees of freedom (nodes), which typically takes about 60 min to cover the frequency range from 10 Hz to

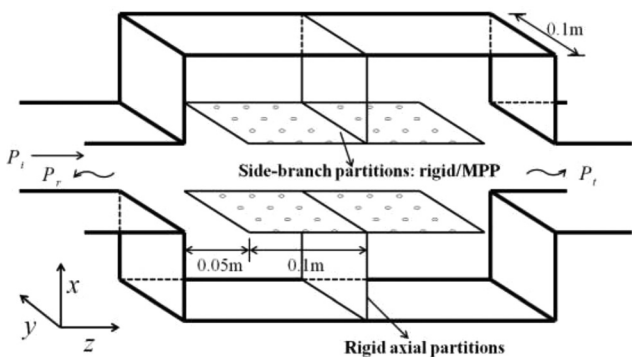

FIG. 12. An example of dual-chamber duct silencer with rigid axial partitions and rigid/MPP side-branch partitions.

Redistribution subject to ASA license or copyright; see http://acousticalsociety.org/content/terms. Download to IP: 158.132.172.70 On: Sat, 10 May 2014 10:08:28

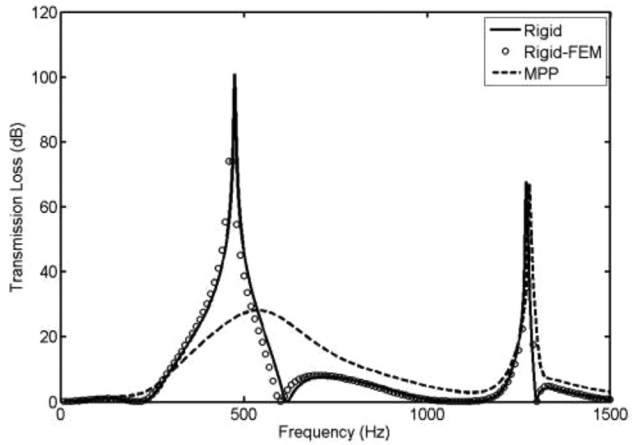

FIG. 13. Comparison of the predicted TLs using the present approach/FEM, and when the side-branch partitions are MPPs.

1500 Hz with a 10 Hz step size, while the present approach reduces the calculation time to <1 min, including the preprocessing time for obtaining subsystem transfer functions.

When MPP side-branch partitions are added, Fig. 13 shows that the introduced MPPs result in a more flattened TL curve, with the first strong peak being suppressed. The smoothened TL peak can plausibly be explained by the weakened resonator effect, which is due to the pressure balance between the two sides of the partitions in the presence of perforation, in agreement with the observation in Sec. III E. On the other hand, the TL trough right after the sharp peak is lifted-up by the MPPs, leading to a widened acoustic stop-band by means of internal absorption through the holes. Together with other evidences shown in the literature regarding silencer design, it can be seen that, upon availability of suitable tools, the silencing performance of the silencers can be tuned or optimized through a proper design of internal arrangement. Under the umbrella of the sub-structuring technique, the proposed virtual panel treatment provides great flexibility in handling such systems, especially in performing possible system optimizations.

IV. CONCLUSION

An equivalent virtual panel treatment is proposed to model thin apertures involved in complex vibroacoustic systems. The proposed method is capable of handling mixed separations/interfaces comprising both structural and acoustic components, allowing sound transmission both structurally and acoustically. The proposed treatment requires the aperture thickness to be sufficiently small compared to the minimum acoustic wavelength. The theoretical formulation of the virtual panel treatment is established, assessed, and validated through comparisons with FEM in two typical examples.

The proposed virtual panel treatment considers the aperture as an equivalent structural component to be integrated with the flexible structure to form a unified compound interface. This greatly simplifies the traditional interface treatment, thus providing an efficient and versatile tool to tackle system complexities when using various sub-structuring techniques. Various examples are investigated, through which the capability of the proposed treatment is demonstrated.

As a rule of thumb, the effective thickness allowing for a satisfactory prediction using virtual panel element is roughly $\lambda_s/4$. Reaching $\lambda_s/16$, the convergence of the calculation can be fully guaranteed, limiting the error at ~0.2%. Typically, for a frequency range up to 10 kHz, the thickness of the virtual panel is required to be smaller than 8.5 mm (corresponding to $\lambda_s/4$).

For illustration purposes, examples involving parallel coupling are also studied to understand the influence of the structural resonances as well as the micro-perforation effects on the coupled acoustic field. The aperture usually dominates the transmission path at most frequencies, while the structural path comes into play when the partial structure undergoes resonances. Micro-perforations also alter the acoustic field mainly by an obvious effect in balancing the acoustic pressure across the MPP panels, and a simultaneous sound absorption effect.

Through numerical examples, the capability and flexibility of the proposed treatment are demonstrated. The versatility of the virtual panel treatment also implies the possibility of performing system optimization. Based on the current formulation, parametric studies can also be conducted to provide guidance when designing such acoustic systems.

It should be noted, however, the current virtual panel formulation is based on the classical wave equation in which visco-thermal effect of the acoustic medium is neglected. For apertures of extremely small size like narrow slits, the visco-thermal effects or acoustic boundary layer effect may become predominant. This needs to be studied in future work.

ACKNOWLEDGMENT

The authors wish to acknowledge a grant from Research Grants Council of Hong Kong Special Administrative Region, China (Grant No. PolyU 5103/13E).

[1]E. H. Dowell, G. F. Gorman, and D. A. Smith, "Acoustoelasticity: General theory, acoustic natural modes and forced response to sinusoidal excitation, including comparisons with experiments," J. Sound Vib. **52**, 519–542 (1977).
[2]E. H. Dowell and H. M. Voss, "The effect of a cavity on panel vibration," AIAA **1**, 476–477 (1963).
[3]L. Cheng and J. Nicolas, "Radiation of sound into a cylindrical enclosure from a point-driven end plate with general boundary conditions," J. Acoust. Soc. Am. **91**, 1504–1513 (1992).
[4]J. Pan, C. H. Hansen, and D. A. Bies, "Active control of noise transmission through a panel into a cavity: I. Analytical study," J. Acoust. Soc. Am. **87**, 2098–2108 (1990).
[5]J. Pan and C. H. Hansen, "Active control of noise transmission through a panel into a cavity. II: Experimental study," J. Acoust. Soc. Am. **90**, 1488–1492 (1991).
[6]L. Cheng, Y. Y. Li, and J. X. Gao, "Energy transmission in a mechanically-linked double-wall structure coupled to an acoustic enclosure," J. Acoust. Soc. Am. **117**, 2742–2751 (2005).
[7]D. Ouellet, J. L. Guyader, and J. Nicolas, "Sound field in a rectangular cavity in the presence of a thin, flexible obstacle by the integral equation method," J. Acoust. Soc. Am. **89**, 2131–2139 (1991).

Redistribution subject to ASA license or copyright; see http://acousticalsociety.org/content/terms. Download to IP: 158.132.172.70 On: Sat, 10 May 2014 10:08:28

[8]O. Beslin and J. L. Guyader, "The use of 'Ectoplasm' to predict radiation and transmission loss of a holed plate in a cavity," J. Sound Vib. **200**, 441–465 (1997).
[9]L. Gagliardini, J. Roland, and J. L. Guyader, "The use of a functional basis to calculate acoustic transmission between rooms," J. Sound Vib. **145**, 457–478 (1991).
[10]G. P. Wilson and W. W. Soroka, "Approximation to the diffraction of sound by a circular aperture in a rigid wall of finite thickness," J. Acoust. Soc. Am. **37**, 286–297 (1965).
[11]M. C. Gomperts and T. Kihlman, "The sound transmission loss of circular and slit-shaped aperture in walls," Acustica **18**, 144–150 (1967).
[12]F. P. Mechel, "The acoustic sealing of holes and slits in walls," J. Sound. Vib. **111**, 297–336 (1986).
[13]F. Sgard, H. Nelisse, and N. Atalla, "On the modeling of the diffuse field sound transmission loss of finite thickness apertures," J. Acoust. Soc. Am. **122**, 302–313 (2007).
[14]N. Trompette, J. L. Barbry, F. Sgard, and H. Nelisse, "Sound transmission loss of rectangular and slit-shaped apertures: Experimental results and correlation with a modal model," J. Acoust. Soc. Am. **125**, 31–41 (2009).
[15]J. Poblet-Puig and A. Rodriguez-Ferran, "Modal-based prediction of sound transmission through slits and openings between rooms," J. Sound. Vib. **332**, 1265–1287 (2013).
[16]H. Huang, X. Qiu, and J. Kang, "Active noise attenuation in ventilation windows," J. Acoust. Soc. Am. **130**, 176–188 (2011).
[17]S. M. Kim, "A compact matrix formulation using the impedance and mobility approach for the analysis of structural and acoustic systems," J. Sound. Vib. **223**, 97–113 (1999).
[18]A. Dijckmans, G. Vermeir, and W. Lauriks, "Sound transmission through finite lightweight multilayered structures with thin air layers," J. Acoust. Soc. Am. **128**, 3513–3524 (2010).
[19]J. D. Chazot and J. L. Guyader, "Prediction of transmission loss of double panels with a patch-mobility method," J. Acoust. Soc. Am. **121**, 267–278 (2007).
[20]X. Yu, L. Cheng, and J. L. Guyader, "Vibroacoustic modeling of cascade panels system involving apertures and micro-perforated elements," in *20th International Congress on Sound and Vibration* (2013).
[21]L. Maxit, C. Yang, L. Cheng, and J. L. Guyader, "Modeling of micro-perforated panels in a complex vibro-acoustic environment using patch transfer function approach," J. Acoust. Soc. Am. **131**, 2118–2130 (2012).
[22]J. Missaoui and L. Cheng, "A combined integro-modal approach for predicting acoustic properties of irregular-shaped cavities," J. Acoust. Soc. Am. **101**, 3313–3321 (1997).
[23]J. Kang and Z. Li, "Numerical simulation of an acoustic window system using finite element method," Acust. Acta Acust. **93**, 152–163 (2007).
[24]J. Pan, "A note on the prediction of sound intensity," J. Acoust. Soc. Am. **93**, 1641–1644 (1993).
[25]E. Anynzoghe and L. Cheng, "On the extension of the integro-modal approach," J. Sound. Vib. **255**, 399–406 (2002).
[26]M. Tournour and N. Atalla, "Pseudostatic corrections for the forced vibroacoustic response of a structure-cavity system," J. Acoust. Soc. Am. **107**, 2379–2386 (2000).
[27]S. M. Kim and Y. H. Kim, "Structural-acoustic coupling in a partially opened plate-cavity system: Experimental observation by using nearfield acoustic holography," J. Acoust. Soc. Am. **109**, 65–74 (2001).
[28]W. L. Li, X. Zhang, J. Du, and Z. G. Liu, "An exact series solution for the transverse vibration of rectangular plates with general elastic boundary supports," J. Sound Vib. **321**, 254–269 (2009).
[29]J. T. Du, W. L. Li, H. A. Xu, and Z. G. Liu, "Vibro-acoustic analysis of a rectangular cavity bounded by a flexible panel with elastically restrained edges," J. Acoust. Soc. Am. **131**, 2799–2810 (2012).
[30]X. N. Wang, Y. S. Choy, and L. Cheng, "Hybrid noise control in a duct using a light micro-perforated plate," J. Acoust. Soc. Am. **132**, 3778–3787 (2012).
[31]A. Selamet and Z. L. Ji, "Acoustic attenuation performance of circular expansion chambers with extended inlet/outlet," J. Sound Vib. **223**, 197–212 (1999).

Redistribution subject to ASA license or copyright; see http://acousticalsociety.org/content/terms. Download to IP: 158.132.172.70 On: Sat, 10 May 2014 10:08:28